Transfusion Medicine and Hemotherapy

Brief Report

Transfus Med Hemother
DOI: 10.1159/000535060

Received: August 4, 2023
Accepted: November 5, 2023
Published online: February 9, 2024

Increase of Phosphoprotein Expressions in Amotosalen/UVA-Treated Platelet Concentrates

Charlotte Muret[a] David Crettaz[a] Lorenzo Alberio[b] Michel Prudent[a, c, d]

[a]Laboratoire de Recherche sur Les Produits Sanguins, Transfusion Interrégionale CRS, Epalinges, Switzerland; [b]Division of Hematology and Central Hematology Laboratory, CHUV, Lausanne University Hospital (CHUV) and University of Lausanne (UNIL), Lausanne, Switzerland; [c]Center for Research and Innovation in Clinical Pharmaceutical Sciences, Lausanne University Hospital (CHUV) and University of Lausanne (UNIL), Lausanne, Switzerland; [d]Institute of Pharmaceutical Sciences of Western Switzerland, University of Geneva, Geneva, Switzerland

Keywords

Pathogen inactivation · Platelet · Phosphoproteomics · Transfusion medicine

Abstract

Background: Pathogen inactivation treatment (PIT) has been shown to alter platelet function, phenotype, morphology and to induce a faster aging of platelet concentrates (PCs). Key pieces of information are still missing to understand the impacts of PITs at the cellular level. ***Objectives:*** This study investigated the impact of amotosalen/UVA on PCs, from a post-translational modifications (PTM) point of view. Phosphoproteomic analyses were conducted on resting platelets, right after the amotosalen/UVA treatment and compared with untreated PCs. ***Method:*** A two-arm study setting was carried out to compare PIT (amotosalen/UVA) to untreated PCs, on day 1 post-donation. Based on a pool-and-split approach, 12 PCs were split into two groups (treated and untreated). Quantitative phosphoproteomics was performed using TMT technology to study the changes of phosphoproteins right after the PIT. ***Results:*** A total of 3,906 proteins and 7,334 phosphosites were identified, and 2,473 proteins and 2,214 phosphosites were observed in at least 5 to 6 replicates. Compared to untreated platelets, PIT platelets exhibited an upregulation of the phosphorylation effects, with 109 phosphosites identified with a higher than 2-fold change. Two pathways were clearly identified. The mitogen activated protein kinases (MAPKs) cascade, which triggers the granule secretion and the activation of the pS15 HSPB1. One of the shape change pathways was also observed with the inhibition of the Threonine 18 and Serine 19 phosphorylations on myosin light chain (MLC) protein after the amotosalen/UVA treatment. ***Conclusions:*** This work provides a deep insight into the impact of amotosalen/UVA treatment from a phosphoprotein viewpoint on resting platelets. Clear changes in phosphorylation of proteins belonging to different platelet pathways were quantified. This discovery corroborates previous findings and fills missing parts of the effect of photochemical treatments on platelets.

Introduction

The implementation of pathogen inactivation technologies (PITs) for platelet concentrates (PCs) has resulted in several advantages in transfusion medicine. It has proven beneficial for patients by reducing transfusion-transmitted infections and transfusion reactions. It also had a positive impact on the blood supply by extending the storage duration from 5 to 7 days.

karger@karger.com
www.karger.com/tmh

Correspondence to:
Michel Prudent, michel.prudent@itransfusion.ch

However, the use of pathogen-inactivated PCs has been known to induce a decrease on the Corrected Count Increment (CCI) values post-transfusion [1–3] and alter in vitro platelet properties [4–7]. Indeed, these photochemical or photo-treatments modify the phenotype and functions of platelets to different extents. Compared to untreated PCs, increased p-selectin expression (platelet activation), exposure of phosphatidylserine (marker of senescence), decrease in GPIb expression (von Willebrand receptor), activation of integrin αIIbβ3 (fibrinogen receptor), modulation of aggregation responses (function of agonists), and modification of metabolite levels have been reported [8–17].

Proteomic analyses revealed a moderate impact of PITs [6] on the around 4,000 proteins of the platelet proteome [18, 19], with an acceleration of storage lesions. Several studies reported the alteration of proteins (different levels of expression, truncation, for instance) [19–21], but modifications of interest were particularly highlighted when looking at post-translational modifications (PTMs) such as oxidation or phosphorylation of proteins. Following both the riboflavin/UV and amotosalen/UVA treatments, p38 mitogen-activated protein kinase (MAPK) was significantly phosphorylated [12, 22]. Protein oxidations were also reported by Johnson and Marks [11] and Sonego et al. [23, 24]. The identified oxidized proteins were involved in platelet shape change and aggregation pathways. These two types of PTMs play a key role since they are linked together, and cross-talks have been demonstrated in several platelet mechanisms [25]. By targeting the oxidation of cysteine moieties (sulfenic acid), we identified an increase of sulfenylated sites, of which Cys412 is in integrin β3, following the amotosalen/UVA treatment [26]. This oxidation is in agreement with the activation of integrin αIIbβ3 and the phosphorylation of p38MAPK [27, 28]. In the present work, we focus on the impact of a PIT, namely amotosalen/UVA, on the phosphoproteome of platelets in the context of transfusion medicine.

Materials and Methods

Platelet Concentrates

PCs were prepared from five pooled buffy coats, each according to standard blood bank procedures in 39% plasma and 61% additive solution (SSP+), as previously described [29]. On day 1 post-donation, 12 PCs from 3 pool-and-split were divided into two groups: treated by amotosalen/UVA and untreated (control). As previously described, Amotosalen/UVA treatment was achieved using the Intercept blood system for platelets [9]. Samples of PCs were withdrawn before (on the pool) and right after the treatment.

Sample Preparation

Five hundred microliters of PCs were mixed with 5 µL of Prostaglandin E1 (Sigma, P5515) at 100 µM and incubated for 10 min prior to a centrifugation step of 500 *g* for 10 min at room temperature. Directly after the centrifugation, the supernatant was removed, and the platelet pellet was snap-frozen in liquid nitrogen prior to being stored at −80°C until analysis.

Quantitative Phosphoproteomics

Trypsin digestion of 120 µg of proteins per sample was done according to the SP3 protocol of Hugues et al. [30]. Peptides were then mixed with 0.4 mg of TMT 10-plex reagents (Thermo Fisher Scientific P/N 90111). Enrichment of phosphopeptides was done by IMAC using the High-Select™ Fe-NTA Phosphopeptide Enrichment Kit (Thermo Fisher Scientific PN A32992). The eluate products were dried and resuspended in 70 µL of 2% acetonitrile and 0.05% trifluoro acetate prior the LC-MS/MS analysis. Tryptic peptide mixtures were analyzed by reversed-phase chromatography with a gradient from 4 to 76% acetonitrile in 0.1% formic acid on an Ultimate RSLC 3000 nanoHPLC. System interface was done via a normal nanospray ion source or a Field Asymmetric Waveform Ion Mobility Spectrometry (FAIMS) on an Orbitrap Fusion Tribrid Mass Spectrometer.

Data Analysis

Raw MS files obtained with FAIMS ion separation were split into independent files relative to each CV using the software Freestyle 1.6.90.0. All tandem MS data were processed by the MaxQuant software (version 1.6.14.0), incorporating the Andromeda search engine. The UNIPROT-SWISSPROT human proteome database of September 2020 (20,371 sequences) was used.

Data Processing and Statistics

R language version 4.2.2 (2022) has been used to perform all statistic tests and graphics. The two groups (control [before the PIT] and treated [directly after the UV treatment]) were compared using a fold change based on a $\log_2$ intensity. Only proteins and phosphosites present at least in 5 out of 6 samples of each group were processed. The phosphosite database has been normalized based on the total protein amount. Significant differences were defined with a p value lower than 0.05, based on a t-test for each phosphosite. Data are presented as mean ± standard deviation (SD). Protein-protein interactions and pathway analysis were additionally performed using string database (www.string-db.org, access on July 2023) and KEGG (www.KEGG.jp, access on July 2023). Data interpretation was supported using the databases Uniprot and phosphositeplus.

Results

Data Processing and Clustering

A total of 3,906 proteins and 7,334 phosphosites were identified. After data processing, it was decided to select only proteins or phosphosites present at least in 5 out of the 6 replicates in each group (control and treated PCs). With these data curation, 2,473 proteins and 2,214 phosphosites were retained (see list in online suppl. Information; for all online suppl. material, see https://doi.org/10.1159/000535060). Descriptive data overview is shown in Figure 1. The histogram shows the pattern of our data, exhibiting a shift to the upregulation of phosphorylation, with a mean of $\log_2(1.12)$ (shown in Fig. 1a). This pattern is also visible on the volcano plot (shown in Fig. 1b). 642 phosphosites were significantly different between the two groups (p value ≤0.05). Thresholds of $-\log_2(1.5)$ and $\log_2(2)$ were selected to significantly

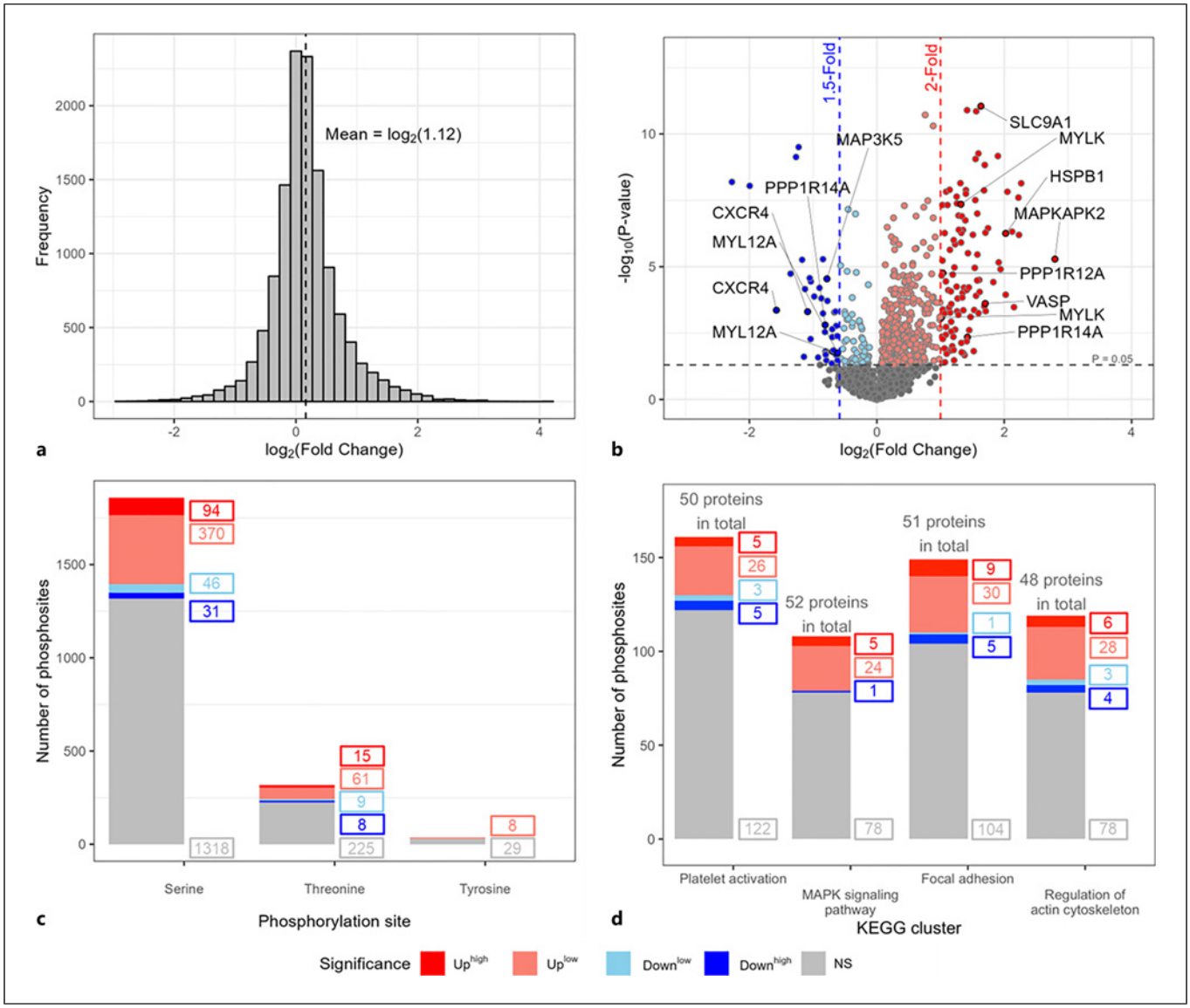

Fig. 1. Data processing visualization and clustering. **a** Histogram showing the frequency of the fold change (FC) based on a $\log_2$ intensity ratio between control and treated PCs (treated/control). A positive FC means an increase of phosphorylation expression after the amotosalen/UVA treatment, while a negative FC indicates a decrease in phosphorylation expression. **b** Volcano plot exposing the significant data (black horizontal dash line) and the two thresholds for the down- (blue dash line) and upregulation (red dash line). **c** Phosphosites frequency in function of the amino acid sites segregated with the different significance groups shown in **b**. **d** Selection of four KEGG pathways with the number of unique proteins with at least one phosphosite observed in our phosphosites data (top of each bar in gray), the number of phosphosites, and the different significance groups are exposed in each bar. Significance is correlated to the FC score; Up^{high} > 2-fold change, 0 < Up^{low} > 2-fold change, 0 > $Down^{low}$ < −1.5-fold change, $Down^{high}$ < −1.5-fold change, and ns value >0.05 *p* value. ns, non-significant.

define phosphosites down- and upregulated. Overall, 94 phosphosites were downregulated, including 39 below the negative threshold, and 548 were upregulated, including 109 above the positive threshold by the PIT. Out of all detected sites, 1,859 took place in a serine residue, while 318 were detected on threonine and 37 on tyrosine (shown in Fig. 1c).

A selection of KEGG clustering was made, as shown in Figure 1d. Four clusters were selected based on the relevance in platelet activation and proteome modification, and on the number of phosphosites and proteins with at least one phosphosite observed. According to the string database, the different KEGG clusters showed the following strength scores: "platelet activation," 0.9; "MAPK signaling pathway," 0.53; "focal adhesion," 0.68; and "regulation of actin cytoskeleton," 0.64. Only the cluster "platelet activation" is specific to platelet mapping proteins; all the other clusters are general to any cell-type. The same protein or phosphosite could be found in different KEGG clusters.

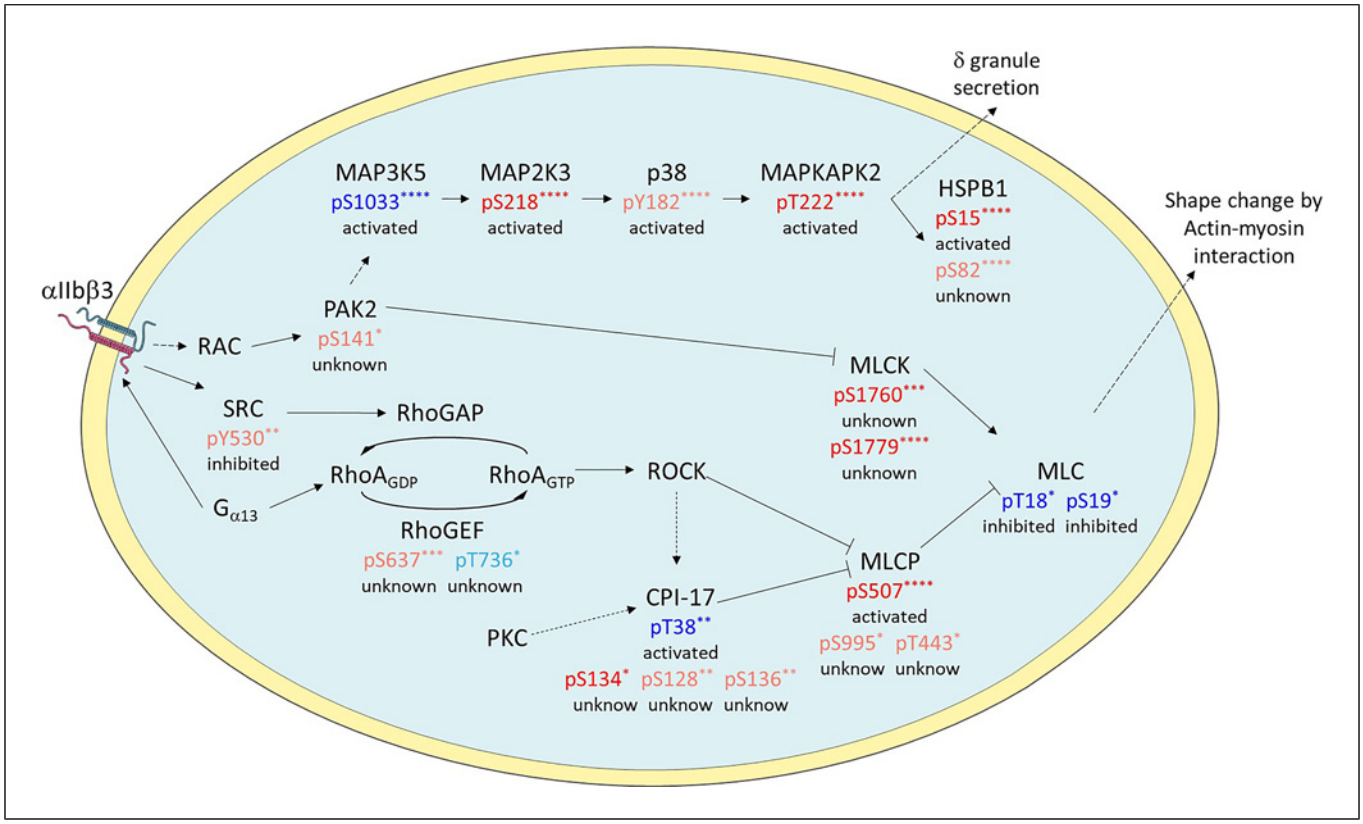

Fig. 2. Impact of amotosalen/UVA treatment on phosphoproteome signaling and platelet pathways. The treatment clearly upregulated the MAPK signaling pathway and inhibited the myosin light chain (MLC) protein involved in regulation of actin cytoskeleton. Each phosphosite is represented in specific color based on the significance, red for upregulation and blue for downregulation after treatment, as defined in Fig. 1. Unknown: impact of the expression on protein activation is unknown, but the phosphosite is known.

Phosphoprotein Modulation in MAP Kinase and Actin Cytoskeleton

Amongst the different protein pathways, the MAP kinase signaling was particularly activated (shown in Fig. 2; Table 1). After treatment, MAP3K5 (Q99683) phosphorylation on S1033 was downregulated. This inactivation phosphosite induced the phosphorylation of MAP2K3 (P46734) on S218, p38MAPK (Q16539) on Y182 and MAPKAPK2 (P49137) on T222, all detected as significantly upregulated in the present study, with a low signal for p38. MAPKAPK2 phosphorylated S15 on HSPB1 (significantly upregulated), and it is also known to activate other pathways (dense granule secretion, for instance) [31] not detected here in this analysis of phosphoprotein signaling.

Significant modulations were also detected within the regulation of actin cytoskeleton (shown in Fig. 2). Phosphorylations on S19 and T18 on myosin light chain (MLC, P19105) were clearly decreased following PIT, inducing a shape change toward a "relaxation" phenotype [32]. This dual phosphorylation is regulated by MLC kinase and phosphatase. The MLC kinase (Q15746) was phosphorylated on S1760 and S1779 in treated PCs. The MLC phosphatase (MYPT1, O14974, as well as other isoforms; see Table 1) was phosphorylated on S507, and low phosphorylation signals of the S995 and T443 were detected. The T696 site, which is inhibited if phosphorylated was detected but not modified by PIT. MLC phosphatase is inhibited by the Rho A activation pathway [33], where only modifications were found on RhoGEF (Q9NZN5) with a low but significant phosphorylation of S637 and a low dephosphorylation of T736. CDI-17(Q96A00), another inhibitor of the MLCP, regulated by Rho-associated protein kinase (ROCK) and protein kinase C (PKC; see Table 1 for phosphosites), shows a dephosphorylation at the T38 site among other phosphorylation sites (high phosphorylation of S134, and low phosphorylation on S128 and S136). The activation of this phosphorylation is known to inhibit MLCP specifically [32]. In addition, other proteins within this pathway were differently expressed upon treatment, such as Na^+/H^+-exchanger 1 (P19634, phosphorylated on S796).

Common to these pathways, the serine/threonine protein kinase 2 (PAK2, Q13177) was phosphorylated on S141. PAK2 is known to inhibit, by phosphorylation, the MLC kinase, which was the case after PIT, where S1760 and S1779 were phosphorylated. In addition, MLC kinase is also activated through the calcium-signaling

Table 1. Summary of phosphosites described in this study

Protein name [gene name (protein number)]	Phosphosite	Mean ± SD significance	Sample size (*N*)	Phospho (S, T, Y) probabilities
RhoGEF [ARHGEF12(Q9NZN5)]	S22	−0.43±0.73 ns	6	HGS(1)ILNR
	S309	0.03±0.47 ns	6	TDCSSGDASRPSSDNADS(1)PK
	S637	0.80±0.32 ***	6	HLSTPS(0.001)S(0.005)VS(0.994)PEPQDSAK
	S1389	0.16±0.51 ns	6	EAHS(1)DENPSEGDGAVNKEEK
	T736	−0.34±0.33 *	6	VTEHGT(1)PKPFR
HSP27 [HSPB1(P04792)]	S15	2.02±0.44 ****	6	GPS(1)WDPFR
	S82	0.89±0.17 ****	6	QLS(0.98)S(0.019)GVSEIR
Integrin α-IIβ [ITGA2B(P08514)]	S427	−0.13±0.51 ns	6	GQVLVFLGQS(1)EGLR
Integrin β-3 [ITGB3(P05106)]	S778	−0.07±0.63 ns	5	EAT(0.02)S(0.951)T(0.02)FT(0.004)NIT(0.004)YR
	T767	0.05±0.17 ns	6	WDT(1)ANNPLYK
	T777	0.08±1.06 ns	6	EAT(0.971)S(0.028)T(0.001)FTNITYR
	T779	0.19±0.76 ns	6	EAT(0.001)S(0.015)T(0.984)FTNITYR
	T781	0.46±0.69 ns	6	EATSTFT(1)NITYR
MAP2K3(P46734)	S218	1.15±0.04 ****	6	MCDFGISGYLVDS(1)VAK
MAP3K5(Q99683)	S1033	−0.78±0.27 ****	6	TLFLGIPDENFEDHSAPPS(1)PEEK
p38 [MAPK14(Q16539)]	Y182	0.46±0.18 ****	6	HTDDEMTGY(1)VATR
MAPKAPK2(P49137)	T222	2.80±0.78 ****	6	ETTSHNS(0.003)LT(0.061)T(0.891)PCY(0.034)T(0.01) PYYVAPEVLGPEK
MLC [MYL12A(P19105)]	S19	−0.69±0.58 *	6	AT(0.016)S(0.984)NVFAMFDQSQIQEFKEAFNMIDQNR
	T18	−0.61±0.53 *	6	AT(0.98)S(0.02)NVFAMFDQSQIQEFK
MYLK(Q15746)	S1760	1.01±0.44 ***	5	LS(0.004)S(0.995)MAMIS(0.001)GLSGR
	S1779	1.32±0.22 ****	6	KSSTGS(0.001)PT(0.049)S(0.95)PLNAEK
	S1848	0.08±0.20 ns	5	IEGYPDPEVVWFKDDQS(1)IR
PAK2(Q13177)	S141	0.16±0.16 *	6	Y(0.001)LS(0.984)FT(0.015)PPEK
	S197	−0.19±0.23 ns	5	S(1)VIDPVPAPVGDSHVDGAAK
	T134	−0.17±0.26 ns	5	FYDS(0.001)NT(0.999)VK
MYPT1 [PPP1R12A(O14974)]	S445	0.19±0.31 ns	6	T(0.001)GS(0.999)YGALAEITASK
	S507	1.04±0.33 ****	6	RLAS(0.996)T(0.004)SDIEEK
	S668	0.21±0.32 ns	5	S(0.996)YLT(0.004)PVRDEESESQR
	S695	−0.07±0.21 ns	5	RS(0.675)T(0.325)QGVTLTDLQEAEK
	S871	0.06±0.33 ns	6	STGVSFWTQDSDENEQEQQS(0.975)DT(0.025)EEGSNKK
	S910	0.25±0.26 ns	5	S(0.005)GS(0.994)YS(0.001)YLEER
	S995	0.44±0.42 *	5	RIS(1)EMEEELK
	T443	0.33±0.35 *	6	T(0.89)GS(0.11)YGALAEITASK
	T696	0.08±0.24 ns	6	RS(0.215)T(0.785)QGVTLTDLQEAEK
CPI-17 [PPP1R14A(Q96A00)]	S128	−0.13±0.25 ns	6	QPS(0.993)PS(0.007)HDGSLSPLQDR
	S128	0.52±0.33 **	5	QPS(0.993)PS(0.007)HDGSLSPLQDR
	S130	0.05±0.47 ns	6	QPS(0.052)PS(0.948)HDGSLSPLQDR
	S134	1.42±0.81 **	5	QPSPSHDGS(0.991)LS(0.008)PLQDR
	S136	0.57±0.34 **	5	QPSPSHDGS(0.006)LS(0.994)PLQDR
	T38	−0.81±0.46 **	6	VT(1)VKYDR
PKA [PRKACA(P17612)]	S339	0.09±0.08 *	6	FKGPGDTSNFDDYEEEEIRVS(1)INEK
	T198	0.11±0.09 *	6	T(0.082)WT(0.915)LCGT(0.003)PEYLAPEIILSK

Table 1 (continued)

Protein name [gene name (protein number)]	Phosphosite	Mean ± SD significance	Sample size (*N*)	Phospho (S, T, Y) probabilities
PKCα[PRKCA(P17252)]	S226	0.01±0.16 ns	6	STLNPQWNES(1)FTFK
	S319	0.60±0.40 **	6	VIS(0.999)PS(0.001)EDR
	T228	0.19±0.45 ns	6	STLNPQWNES(0.02)FT(0.98)FK
	T497	0.13±0.07 **	6	T(1)FCGTPDYIAPEIIAYQPYGK
PKCβ[PRKCB(P05771)]	T500	0.12±0.10 *	6	T(1)FCGTPDYIAPEIIAYQPYGK
	T642	0.00±0.25 ns	5	QPVELT(1)PTDK
	T644	0.18±0.34 ns	5	QPVELT(0.268)PT(0.732)DK
PKCδ[PRKCD(Q05655)]	S130	−0.23±0.49 ns	6	VLMSVQYFLEDVDCKQS(1)MR
	S304	0.26±0.08 ****	6	RS(0.007)DS(0.979)AS(0.014)SEPVGIYQGFEK
	S645	−0.12±0.19 ns	6	ARLS(1)YSDK
	S645	0.09±0.24 ns	6	ARLS(1)YSDK
	S647	0.04±0.33 ns	6	LS(0.358)YS(0.642)DKNLIDSMDQSAFAGFS(1)FVNPK
	S664	0.09±0.23 ns	6	ARLS(0.977)YS(0.023)DKNLIDSMDQSAFAGFS(1)FVNPK
	S664	0.13±0.14 ns	6	ARLS(0.977)YS(0.023)DKNLIDSMDQSAFAGFS(1)FVNPK
	T141	0.18±0.16 *	6	SEDEAKFPT(1)MNRR
	T507	0.11±0.06 **	6	AS(0.104)T(0.896)FCGTPDYIAPEILQGLK
	Y64	0.04±0.62 ns	6	STFDAHIY(1)EGR
PKCθ[PRKCQ(A0A087X0I9)]	S640	−0.05±0.07 ns	6	EFLNEKPRLS(1)FADR
	S659	0.04±0.18 ns	6	NFS(1)FMNPGMER
	T502	0.16±0.09 **	6	T(0.131)NT(0.869)FCGTPDYIAPEILLGQK
ROCK1(Q13464)	S1341	−0.26±0.46 ns	6	STANQS(1)FR
ROCK2(O75116)	S425	0.00±0.81 ns	5	ENLLLS(0.038)DS(0.96)PS(0.002)CR
	S1374	−0.28±0.61 ns	6	IQQNQS(1)IR
	T1212	0.40±0.80 ns	6	LFHVRPVT(1)QTDVYR
SRC(P12931)	S17	0.20±0.37 ns	6	S(1)LEPAENVHGAGGGAFPASQTPSKPASADGHR
	S104	0.00±0.17 ns	6	TETDLS(1)FK
	Y530	0.23±0.16 **	6	KEPEERPTFEYLQAFLEDYFTSTEPQY(1)QPGENL
SNAP23(O00161)	S20	0.00±0.38 ns	6	AHQITDES(0.999)LESTRR
	S110	0.24±0.13 **	6	TTWGDGGENS(1)PCNVVSK
Sodium/hydrogen exchanger 1 [SLC9A1(P19634)]	S599	0.05±0.48 ns	6	IPS(0.999)AVS(0.001)TVSMQNIHPK
	S605	0.14±0.41 ns	6	IPSAVSTVS(0.999)MQNIHPK
	S693	0.13±0.19 ns	6	LDS(0.997)PT(0.003)MSR
	T695	0.18±0.28 ns	6	LDS(0.297)PT(0.701)MS(0.002)R
	S703	0.51±0.33 **	6	IGS(1)DPLAYEPK
	S785	0.12±0.29 ns	6	SKETSSPGTDDVFTPAPS(0.035)DS(0.956)PS(0.008)S(0.002)QR
	S796	1.63±0.11 ****	6	CLS(1)DPGPHPEPGEGEPFFPK
VASP(P50552)	S46	0.09±0.25 ns	6	VQIYHNPTANS(1)FR
	S239	0.09±0.12 ns	6	KVS(1)KQEEASGGPTAPK
	S305	−0.49±1.10 ns	6	VPAQSES(1)VRRPWEK
	S322	1.70±0.75 ***	6	MKS(0.913)S(0.058)S(0.027)S(0.002)VTTSETQPCTPSSSDYSDLQR
	T278	−0.11±0.33 ns	6	KAT(1)QVGEK
	T316	0.10±0.19 ns	5	NST(0.017)T(0.983)LPR
	Y39	−0.02±0.32 ns	6	VQIY(1)HNPTANSFR

Table 1 (continued)

Protein name [gene name (protein number)]	Phosphosite	Mean ± SD significance	Sample size (*N*)	Phospho (S, T, Y) probabilities
CXCR4(P61073)	S319	−1.09±0.53 ***	6	TSAQHALT(0.066)S(0.933)VSR
	T318	−1.58±0.75 ***	6	TSAQHALT(0.983)S(0.016)VS(0.001)R
PLCB2(Q00722)	S958	0.10±0.13 ns	6	S(1)LPREESAGAAPGEGPEGVDGR
ITPR1(A0A3B3IU04)	S1589	0.04±0.11 ns	6	RDS(1)VLAASR
	S1194	−0.01±0.60 ns	6	LCVQES(0.112)AS(0.888)VRK
	S1568	−0.20±0.24 ns	6	SHS(1)IVQK
	S1755	0.13±0.15 ns	5	RES(0.999)LT(0.001)SFGNGPLSAGGPGK

For each specific phosphosite detected, mean ± SD of $\log_2$(fold change), significance, sample size and the sequence with the phosphosite localization were added. ns, non-significant. *p* value of *: <0.05, **: <0.01, ***: <0.001, ****: <0.0001.

pathway. Despite downregulation of T318 and S319 on CXCR4 (P61073), the other intermediate proteins along that chain (PLCβ2 [Q00722] and ITPR1 [Q14643]) did not show any modification on detected phosphosites. On the other side, PAK2 was reported to trigger, through S141 phosphorylation, different signaling pathways, which could explain the MAPK cascade observed here.

Regarding platelet activation, in addition to the above-cited proteins, protein kinase A (PKA, P17612) and its target vasodilator-stimulated phosphoprotein (VASP, P50552) were significantly phosphorylated on S339 and T198 (required for activation) and S322 (well-known modification), respectively. Synaptosomal-associated protein 23 (SNAP23, O00161) inducing exocytosis when phosphorylated, i.e., release of granules, was upregulated on phospho-S110.

Discussion

Photo- or photochemical treatments to inactivate pathogens in PCs have been known to modify platelet properties [8–11, 13–16, 34–36]. Of interest, PTMs are regulated by PITs, as shown by the phosphorylation of p38MAPK by both Intercept [12] and Mirasol [22] treatments; although moderate, this increase was significant. The present work focused on the impact of amotosalen/UVA treatment from a basal platelet stage perspective. 3,906 proteins and 7,334 phosphosites were detected and quantified, which is similar to the results of Burkhart and colleagues [18] with their 4,000 unique proteins and in agreement with the literature [19, 26]. As it was decided to be restrictive and to consider only proteins and phosphosites present in at least 5 over 6 replicates, the curation ended up with 2,473 proteins and 2,214 phosphosites. The amotosalen/UVA treatment increases the global phosphorylation of proteins, as shown in Figures 1a, b, with 94 significantly downregulated versus 548 significantly upregulated sites. In the same line, the selection of KEGG clusters exhibits an upregulation pattern for all four groups. Despite the limited understanding of a few proteins, the present in-depth phosphoproteome analysis demonstrated a clear shift of phosphorylation expression in resting platelets following the amotosalen/UVA treatment.

A definite modulation was observed within the MAPK signaling pathway. The p38MAPK phosphorylation was reported within the cascade from MAP3K5 to the heat shock protein (HSPB1). This cascade participates in integrin activation and aggregation, dense granule secretion, and microvesicle release in platelets [5, 31, 34]. We hypothesized that the activation of p38 within the integrin αIIbβ3 pathway could be a consequence of integrin β3 oxidation on Cys due to amotosalen/UVA treatment [26], a process known to induce oxidations [24, 35, 36]. This cross-talk between oxidation and phosphorylation could activate the MAPK cascade through PAK2 phosphorylation. The activation pathway between integrin β3 and PAK2 via RAC1 and other proteins [27, 33, 37] has yet to be deciphered and other PTMs could be involved.

The platelet shape change between a "contraction" and a "relaxation" state is modulated by two pathways through Rho GTPases [32], where the phosphorylation of the S19 MLC by the MLC kinase will induce the contraction of the platelet [32, 33], and the inhibition of the MLC phosphatase will increase the S19 phosphorylation [33]. The opposite pathway is the MLC phosphatase that regulates the relaxation of the platelet by the dephosphorylation of the MLC [32, 38].

The MLC phosphatase appeared upregulated in our data set, despite identical levels of phosphorylation on T696 in both conditions, which is known to be a key player on the activation of the MLCP [39], since another activation site was upregulated. In fact, the MYPT1 S507 (O14974, an MLC phosphatase detected here) was phosphorylated, suggesting an activation of the MLCP inducing a dephosphorylation of the MLC [38]. A known regulator of the phosphatase is the RhoA pathway, which

exhibited low levels of modulation by the treatment here, where only two sites were significantly regulated in the RhoGEF pathway (with a low upregulation of S637 and with a low downregulation of T736). Another phosphatase inhibitor is the CPI-17, which is regulated by the ROCK and PKC pathways in smooth muscle contraction [40]. Phosphorylation of CPI-17 T38 inhibits the MLCP and promotes platelet contraction [32]. Moreover, Kitazawa and colleagues [39] showed that the dephosphorylation of the CPI-17 at T38 could be correlated with the activation of the MLCP and with the dephosphorylation of the MLC in smooth muscle. These results corroborate the one found in this study, with the dephosphorylation of T38 CPI-17, the phosphorylation of S507 MLCP, and the dephosphorylation of the MLC, triggered by PIT.

As for the MLC kinase, it appeared to be phosphorylated in two sites (S1760 and S1779), but their impact on the MLC is unclear. The kinase is activated via the calcium-signaling pathway. Except for a modification on CXCR4, no other calcium-signaling modification was detected at the phosphoprotein level, suggesting an activation of this kinase from PAK2. This hypothesis agrees with the modulation of MLC in the integrin outside-in signaling from Flevaris et al. [27], where the activation could be triggered by oxidation on integrin [26, 28].

All taken together, the clear inhibition of MLC (dephosphorylation following PIT) is expected to be triggered by the inhibition of the MLC kinase and/or the activation of MLC phosphatase. At last, the impact of the intracellular calcium on the MLCK and MLCP pathways is still unclear and needs to be deciphered [32, 39].

Clinical trials and meta-analyses have revealed a moderate impact following the transfusion of pathogen-inactivated PCs compared to untreated PCs. A decrease in CCI with or without impact on PC consumption has been reported [1–3]. This observation might be explained by an increase of PS expression, platelet activation, and GPIb shedding, as mentioned in Introduction [4–17]. The activation of the MAPK pathway is in agreement with this phenotype, where p38 phosphorylation is induced by amotosalen/UVA treatment and related to PS expression and GPIb shedding that primes this receptor for cleavage. As for MLC, the decrease in phosphorylation alters the clot retraction [27]. Altered clot retraction might induce bleeding, but pathogen-inactivated PCs have not been associated with increased bleeding events [2, 3]. As a limitation, the present work focused on the impact of amotosalen/UVA treatment at a specific time point from a basal platelet state. The evolution of these phosphosites after transfusion remains unknown. The clinical interpretation of such omic studies goes thus beyond the scope of the presented data. Nevertheless, it enabled us to identify biomarkers that should be included in further functional assays during clinical investigations.

In summary, this work provides a deep insight into the impact of amotosalen/UVA treatment from a phosphoprotein viewpoint at the basal stage of the platelets. Even though this PIT has shown limited platelet function alterations [9, 41] compared to others [8], we were able to observe clear changes in the expression of phosphorylation in proteins belonging to different platelet pathways. At the cellular level, the amotosalen/UVA treatment might alter the chaperon activity for protein folding (see HSPB1), actin-myosin assembly and platelet shape change (see regulation of MLC), and granule secretion (see regulation of MAPKAPK2 and p38 activation). Despite the protein-oriented information, this work corroborates previous findings and fills missing parts in the effect of photochemical treatments on platelets.

Acknowledgments

Dr. Manfredo Quadroni and the Protein Analysis Facility collaborators (UNIL, Lausanne) are thanked for their technical support and the acquisition of phosphoproteomic data. The insightful discussions regarding sample preparation with Dr. Alessandro Aliotta were also highly thanked.

Statement of Ethics

Informed consent was obtained from all subjects involved in the study. The study was in accordance with national legislation and the Institutional Review Board of Transfusion Interrégionale CRS. Ethical approval was not required for this study in accordance with national guidelines and the institutional requirement.

Conflict of Interest Statement

The authors have no conflicts of interest to declare.

Funding Sources

This work was supported by the Swiss Red Cross humanitarian foundation (#254).

Author Contributions

Charlotte Muret and Michel Prudent designed the experiments, interpreted the data, and wrote the manuscript. Charlotte Muret and David Crettaz carried out the experiments. Charlotte Muret treated the data. Lorenzo Alberio reviewed the data and the manuscript. Lorenzo Alberio and Michel Prudent supervised the project and obtained the funding.

Data Availability Statement

All data generated or analyzed during this study are included in this article. Further inquiries can be directed to the corresponding author.

References

1 Infanti L, Holbro A, Passweg J, Bolliger D, Tsakiris DA, Merki R, et al. Clinical impact of amotosalen-ultraviolet A pathogen-inactivated platelets stored for up to 7 days. Transfusion. 2019;59(11):3350–61.
2 Pati I, Masiello F, Pupella S, Cruciani M, De Angelis V. Efficacy and safety of pathogen-reduced platelets compared with standard apheresis platelets: a systematic Review of RCTs. Pathogens. 2022;11(6):639.
3 Estcourt LJ, Malouf R, Hopewell S, Trivella M, Doree C, Stanworth SJ, et al. Pathogen-reduced platelets for the prevention of bleeding. Cochrane Database Syst Rev. 2017;7(7):CD009072.
4 Feys HB, Van Aelst B, Compernolle V. Biomolecular consequences of platelet pathogen inactivation methods. Transfus Med Rev. 2019;33(1):29–34.
5 Schubert P, Johnson L, Marks DC, Devine DV. Ultraviolet-based pathogen inactivation systems: untangling the molecular targets activated in platelets. Front Med. 2018;5:129.
6 Prudent M, D'Alessandro A, Cazenave JP, Devine DV, Gachet C, Greinacher A, et al. Proteome changes in platelets after pathogen inactivation: an interlaboratory consensus. Transfus Med Rev. 2014;28(2):72–83.
7 Prudent M. What about platelet function in platelet concentrates? Hamostaseologie. 2020;40(4):500–8.
8 Malvaux N, Defraigne F, Bartziali S, Bellora C, Mommaerts K, Betsou F, et al. In vitro comparative study of platelets treated with two pathogen-inactivation methods to extend shelf life to 7 days. Pathogens. 2022;11(3):343.
9 Abonnenc M, Sonego G, Kaiser-Guignard J, Crettaz D, Prudent M, Tissot JD, et al. In vitro evaluation of pathogen-inactivated buffy coat-derived platelet concentrates during storage: psoralen-based photochemical treatment step-by-step. Blood Transfus. 2015;13(2):255–64.
10 Abonnenc M, Sonego G, Crettaz D, Aliotta A, Prudent M, Tissot JD, et al. In vitro study of platelet function confirms the contribution of the Ultraviolet B (UVB) radiation in the lesions observed in riboflavin/UVB-treated platelet concentrates. Transfusion. 2015;55(9):2219–30.
11 Johnson L, Marks D. Treatment of platelet concentrates with the Mirasol pathogen inactivation system modulates platelet oxidative stress and NF-κB activation. Transfus Med Hemother. 2015;42(3):167–73.
12 Stivala S, Gobbato S, Infanti L, Reiner MF, Bonetti N, Meyer SC, et al. Amotosalen/ultraviolet a pathogen inactivation technology reduces platelet activatability, induces apoptosis and accelerates clearance. Haematologica. 2017;102(10):1650–60.
13 Jóhannsson F, Árnason NÁ, Landrö R, Guðmundsson S, Sigurjonsson ÓE, Rolfsson Ó. Metabolomics study of platelet concentrates photochemically treated with amotosalen and UVA light for pathogen inactivation. Transfusion. 2020;60(2):367–77.
14 Bertaggia Calderara D, Crettaz D, Aliotta A, Barelli S, Tissot JD, Prudent M, et al. Generation of procoagulant collagen- and thrombin-activated platelets in platelet concentrates derived from buffy coat: the role of processing, pathogen inactivation, and storage. Transfusion. 2018;58(10):2395–406.
15 Leitner GC, Hagn G, Niederstaetter L, Bileck A, Plessl-Walder K, Horvath M, et al. INTERCEPT pathogen reduction in platelet concentrates, in contrast to gamma irradiation, induces the formation of trans-arachidonic acids and affects eicosanoid release during storage. Biomolecules. 2022;12(9):1258.
16 Abonnenc M, Tissot JD, Prudent M. General overview of blood products in vitro quality: processing and storage lesions. Transfus Clin Biol. 2018;25(4):269–75.
17 Chavarin P, Cognasse F, Argaud C, Vidal M, De Putter C, Boussoulade F, et al. In vitro assessment of apheresis and pooled buffy coat platelet components suspended in plasma and SSP+ photochemically treated with amotosalen and UVA for pathogen inactivation (INTERCEPT Blood System). Vox Sang. 2011;100(2):247–9.
18 Burkhart JM, Vaudel M, Gambaryan S, Radau S, Walter U, Martens L, et al. The first comprehensive and quantitative analysis of human platelet protein composition allows the comparative analysis of structural and functional pathways. Blood. 2012;120(15):e73–82.
19 Aloui C, Barlier C, Claverol S, Fagan J, Awounou D, Tavernier E, et al. Differential protein expression of blood platelet components associated with adverse transfusion reactions. J Proteomics. 2019;194:25–36.
20 Prudent M, Crettaz D, Delobel J, Tissot JD, Lion N. Proteomic analysis of Intercept-treated platelets. J Proteomics. 2012;76 Spec No:316–28.
21 Salunkhe V, De Cuyper IM, Papadopoulos P, van der Meer PF, Daal BB, Villa-Fajardo M, et al. A comprehensive proteomics study on platelet concentrates: platelet proteome, storage time and Mirasol pathogen reduction technology. Platelets. 2019;30(3):368–79.
22 Schubert P, Coupland D, Culibrk B, Goodrich RP, Devine DV. Riboflavin and ultraviolet light treatment of platelets triggers p38MAPK signaling: inhibition significantly improves in vitro platelet quality after pathogen reduction treatment. Transfusion. 2013;53(12):3164–73.
23 Sonego G, Abonnenc M, Crettaz D, Lion N, Tissot JD, Prudent M. Irreversible oxidations of platelet proteins after riboflavin-UVB pathogen inactivation. Transfus Clin Biol. 2020;27(1):36–42.
24 Prudent M, Sonego G, Abonnenc M, Tissot JD, Lion N. LC-MS/MS analysis and comparison of oxidative damages on peptides induced by pathogen reduction technologies for platelets. J Am Soc Mass Spectrom. 2014;25(4):651–61.
25 Sonego G, Abonnenc M, Tissot JD, Prudent M, Lion N. Redox proteomics and platelet activation: understanding the redox proteome to improve platelet quality for transfusion. Int J Mol Sci. 2017;18(2):387.
26 Sonego G, Le TTM, Crettaz D, Abonnenc M, Tissot JD, Prudent M. Sulfenylome analysis of pathogen-inactivated platelets reveals the presence of cysteine oxidation in integrin signaling pathway and cytoskeleton regulation. J Thromb Haemost. 2021;19(1):233–47.
27 Flevaris P, Li Z, Zhang G, Zheng Y, Liu J, Du X. Two distinct roles of mitogen-activated protein kinases in platelets and a novel Rac1-MAPK-dependent integrin outside-in retractile signaling pathway. Blood. 2009;113(4):893–901.
28 Yan B, Smith JW. Mechanism of integrin activation by disulfide bond reduction. Biochemistry. 2001;40(30):8861–7.
29 Muret C, Crettaz D, Martin A, Aliotta A, Bertaggia Calderara D, Alberio L, et al. Two novel platelet biotinylation methods and their impact on stored platelet concentrates in a blood bank environment. Transfusion. 2022;62(11):2324–33.
30 Hughes CS, Moggridge S, Müller T, Sorensen PH, Morin GB, Krijgsveld J. Single-pot, solid-phase-enhanced sample preparation for proteomics experiments. Nat Protoc. 2019;14(1):68–85.
31 Patel P, Naik UP. Platelet MAPKs-a 20+ year history: what do we really know? J Thromb Haemost. 2020;18(9):2087–102.
32 Reddi BA, Iannella SM, O'Connor SN, Deane AM, Willoughby SR, Wilson DP. Attenuated platelet aggregation in patients with septic shock is independent from the activity state of myosin light chain phosphorylation or a reduction in Rho kinase-dependent inhibition of myosin light chain phosphatase. Intensive Care Med Exp. 2015;3(1):37.
33 Aslan JE. Platelet shape change; 2017. p. 321–36.
34 Chen Z, Schubert P, Bakkour S, Culibrk B, Busch MP, Devine DV. p38 mitogen-activated protein kinase regulates mitochondrial function and microvesicle release in riboflavin- and ultraviolet light-treated apheresis platelet concentrates. Transfusion. 2017;57(5):1199–207.
35 Abonnenc M, Crettaz D, Tacchini P, Di Vincenzo L, Sonego G, Prudent M, et al. Antioxidant power as a quality control marker for completeness of amotosalen and ultraviolet A photochemical treatments in platelet concentrates and plasma units. Transfusion. 2016;56(7):1819–27.
36 Lotens A, Abonnenc M, Malvaux N, Schuhmacher A, Prudent M, Rapaille A. Antioxidant power measurement in platelet concentrates treated by two pathogen inactivation systems in different blood centres. Vox Sang. 2021;116(1):53–9.
37 Aslan JE, McCarty OJ. Rho GTPases in platelet function. J Thromb Haemost. 2013;11(1):35–46.
38 Ojiaku CA, Cao G, Zhu W, Yoo EJ, Shumyatcher M, Himes BE, et al. TGF-β1 evokes human airway smooth muscle cell shortening and hyperresponsiveness via Smad3. Am J Respir Cell Mol Biol. 2018;58(5):575–84.
39 Kitazawa T, Semba S, Huh YH, Kitazawa K, Eto M. Nitric oxide-induced biphasic mechanism of vascular relaxation via dephosphorylation of CPI-17 and MYPT1. J Physiol. 2009;587(Pt 14):3587–603.

40 Alvarez-Santos MD, Álvarez-González M, Estrada-Soto S, Bazán-Perkins B. Regulation of myosin light-chain phosphatase activity to generate airway smooth muscle hypercontractility. Front Physiol. 2020; 11:701.
41 Hechler B, Ohlmann P, Chafey P, Ravanat C, Eckly A, Maurer E, et al. Preserved functional and biochemical characteristics of platelet components prepared with amotosalen and ultraviolet A for pathogen inactivation. Transfusion. 2013;53(6): 1187–200.
42 Abonnenc M, Crettaz D, Sonego G, Escolar G, Tissot JD, Prudent M. Towards the understanding of the UV light, riboflavin and additive solution contributions to the in vitro lesions observed in Mirasol®-treated platelets. Transfus Clin Biol. 2019;26(4): 209–16.
43 Stivala S, Gobbato S, Infanti L, Reiner MF, Bonetti N, Meyer SC, et al. In response to the comment by Hechler et al.: amotosalen/UVA pathogen inactivation technology reduces platelet activatability, induces apoptosis and accelerates clearance. Haematologica, 2017; 102(12):e504–5.